(20) Viscosity data taken from: "Technical Data Book-Petroleum Refining", 2nd ed.; American Petroleum Institute: Washington, DC, 1970; p 11A2.8.
(21) The activation energy derived in this manner for benzene is 3.05 kcal/mol.[22]
(22) Grotewold, J.; Soria, D.; Previtali, C. M.; Scaiano, J. C. *J. Photochem.* **1972/1973**, *1*, 471.
(23) Terenin, A.; Ermolaev, V. *Trans. Faraday Soc.* **1956**, *52*, 1042.
(24) Förster, Th. *Discuss. Faraday Soc.* **1959**, *27*, 7.
(25) Turro, N. J. *Pure Appl. Chem.* **1977**, *49*, 405.
(26) Klöpffer, W. *Spectrosc. Lett.* **1978**, *11*, 863.
(27) Breslow, R.; Winnik, M. A. *J. Am. Chem. Soc.* **1969**, *91*, 3083.
(28) Maharaj, U.; Winnik, M. A.; Dors, B.; Schäfer, H. J. *Macromolecules* **1979**, *12*, 905. Winnik, M. A.; Hsiao, C.-K. *Ibid.* **1975**, *33*, 518. Winnik, M. A.; Lee, C. K.; Basu, S.; Saunders, D. S. *J. Am. Chem. Soc.* **1974**, *96*, 6182. Winnik, M. A.; Trueman, R. E.; Jackowski, G.; Sunders, D. S.; Whittington, S. G. *Ibid.* **1974**, *96*, 4843.
(29) Breslow, R.; Kitabatake, S.; Rothbard, J. *J. Am. Chem. Soc.* **1978**, *100*, 8156. Czarnieckei, M. F.; Breslow, R. *Ibid.* **1979**, *101*, 3675.
(30) E.g.: Almgren, M.; Grieser, F.; Thomas, J. K. *J. Am. Chem. Soc.* **1979**, *101*, 279. Infelta, P. P.; Grätzel, M.; Thomas, J. K. *J. Phys. Chem.* **1974**, *78*, 190. Thomas, J. K.; Grieser, F.; Wong, M. *Ber. Bunsenges. Phys. Chem.* **1978**, *82*, 937.
(31) E.g.: Yekta, A.; Aikawa, M.; Turro, N. J. *Chem. Phys. Lett.* **1979**, *63*, 543. Aikawa, M.; Yekta, A.; Turro, N. J. *Ibid.* **1979**, *68*, 285.
(32) For a table with the data see ref 12.
(33) E.g.: Herkstroeter, W. G.; Hammond, G. S. *J. Am. Chem. Soc.* **1966**, *88*, 4769.
(34) It is interesting to note that the effect of temperature on k_{iet} may be partially offset by the change in solubility which accompanies the change in temperature.
(35) Freedman, H. H.; Mason, J. P.; Medalia, A. I. *J. Org. Chem.* **1958**, *23*, 76.
(36) Scaiano, J. C. *J. Am. Chem. Soc.* **1980**, *102*, 7747. Encinas, M. V.; Scaiano, J. C. *Ibid.* **1979**, *101*, 2146.

Causes of Haze of Low-Density Polyethylene Blown Films

Ferdinand C. Stehling,* C. Stanley Speed, and Lowell Westerman

Plastics Technology Division, Exxon Chemical Company, Baytown, Texas 77520.
Received June 19, 1980

ABSTRACT: Static and on-line haze, low-angle light scattering, and microscopic measurements have shown that haze of low-density polyethylene (LDPE) blown film is caused mainly by scattering from rough film surfaces. The rough surfaces are formed by two mechanisms, one involving melt flow disturbances at the die exit and the other caused by stress-induced crystallization close to the film surface. Haze arising from melt flow disturbances can be reduced by selecting resins that contain relatively low concentrations of large molecules and by intense mechanical deformation of the melt before extrusion. Mechanical deformation reduces melt elasticity and haze by a reversible physical mechanism that generates a long-lived nonequilibrium melt structure. Haze arising from crystallization may possibly be reduced by introducing more irregularity into the polymer chain by copolymerization or by increasing short-chain branching.

Introduction

Low-density polyethylene (LDPE), made by the free radical initiated polymerization of ethylene at high pressure, is extensively used in the form of film. These films have a more or less milky white or hazy appearance caused by light scattering by the films. In spite of the importance of haze in end-use applications, there is little published information on the mechanisms and causes of haze development in films. The purpose of our work was to acquire a better understanding of the causes of haze of LDPE films, especially blown films. Improved understanding should provide a guide for modifying polymer chain structure and film fabrication conditions to achieve lower haze levels.

When a polymer film is placed in the path of a light beam, light scattering can originate from the interior of the film and from the air–film interfaces. Light scattering from the interior of films made from semicrystalline polymers has been placed on a firm theoretical and experimental basis by Stein[1] and others.[2] In most investigations, scattering from film surfaces has been reduced to negligibly low levels by coating the film with a fluid with a refractive index equal to that of the film or by crystallizing the film between smooth glass microscope slides. Light scattering from film surfaces has been much less extensively examined. However, there is general agreement that the haze of thin ($\sim$25 μm) blown LDPE film is caused mainly by scattering from rough film surfaces.[3-6]

In a classic study, Huck and Clegg[3] examined the effect of extrusion conditions on the haze of blown LDPE films. They interpreted their results in terms of two mechanisms for generating rough film surfaces. These mechanisms give rise to "extrusion haze" and "crystallization haze". In the extrusion haze mechanism, surface bumps were assumed to form on the molten film surface upon exit of the polymer fluid from the film die. The surface bumps were thought to smoothen upon moving downstream from the die until solidification of the film prevented further smoothening. Crystallization haze was postulated to occur from surface roughening caused by the formation of crystalline aggregates on or close to the surface of the film. Using these hypotheses, they rationalized many of the effects of film fabrication conditions on film haze.

A number of workers have proposed that polymer melt elasticity is closely related to blown film haze. According to Huck and Clegg,[3] the haze of LDPE film increases as extrudate die swell increases. Shroff et al. used entrance pressure drop upon flow into a capillary, P_0, as a measure of melt elasticity and concluded that the haze of blown poly(ethylene-*co*-vinyl acetate) film increased as P_0 increased.[7]

The effect of polymer chain structure on LDPE film haze has been only briefly investigated. Perron and Lederman concluded from GPC examination of a few LDPE resins that broadening molecular weight distribution caused an increase in haze.[4] However, no allowance was made for long-chain branching of LDPE in the analysis of the GPC chromatograms, so this conclusion is not firmly established. Foster concluded that the total haze of LDPE blown films increased as the number of long branches in the resin increased.[6]

It is well-known that the haze of LDPE film can be reduced by subjecting the polymer melt to a mechanical deformation in an intensive mixer before extrusion.[8] In the film industry this process is referred to in various ways, such as "working", "homogenization", and "shear refining".

0024-9297/81/2214-0698$01.25/0

Although some of these terms imply a mechanism for haze reduction, the mechanism is poorly understood. We will therefore use the less committal term "mechanical treatment" for this process.

Howells and Benbow reported, without giving supporting data, that mechanical treatment reduced LDPE melt elasticity without attendant molecular weight changes.[9] A similar but better documented conclusion was obtained by Fujiki[5] and Rokudai,[10] who further noted that reduction in elasticity (die swell and entrance pressure drop) was accompanied by a decrease in film haze.[10] Howells and Benbow stated that the reduction in elasticity could be almost completely reversed by holding the melt at high temperatures for long times and by dissolving and reprecipitating the polymer, but no data to support these assertions were given.[9] They interpreted the reduction and recovery of elasticity in terms of a reversible disentanglement–reentanglement mechanism. Mechanical deformation effects analogous to those described above for LDPE were also found for branched poly(oxymethylene) by Prichard and Wissbrun.[11] These investigators reported that repeated extrusion decreased extrudate swell and the die entrance correction for capillary flow, but it did not effect viscosity. Linear poly(oxymethylene) showed much smaller effects upon reextrusion. On the other hand, Albright attributed the reduction of film haze resulting from mechanical deformation of the melt to polymer chain scission, but he presented no data to support this view.[8] Hanson concluded that mechanical deformation of molten LDPE could cause both chain scission and partly reversible changes in die swell.[12]

The specific objectives of our work were to establish the mechanisms for haze formation in blown LDPE film, to determine the effect of polymer chain structure on film haze, and to determine the reason why mechanical deformation of the polymer melt reduces haze. All previously reported haze studies have involved examination of films *after* film fabrication. The thrust of our work was to also make measurements *during* film fabrication so that haze could be observed as it developed. We have used a number of different methods for examining films, including haze measurements, small-angle light scattering (SALS), and microscopic examination to minimize the possibility of drawing incorrect conclusions.

Experimental Section

The resins used in this work, together with characterization data, are listed in Table I. The LDPE resins were all homopolymers made by the free radical initiated polymerization of ethylene at high pressures, and they contained no additives other than very small concentrations of an oxidation inhibitor. A single high-density polyethylene, designated as HD-0, was also examined. Melt index was determined by a procedure described in ASTM standard method D1238-70, condition E. Density was measured by using a water–2-propanol density gradient column on melt index extrudates that had been annealed for 1 h at 100 °C. Characterization of the molecular structure (long-chain branching and molecular weight) was accomplished by using a GPC–intrinsic viscosity procedure described previously.[13–15] Molecular weight averages given are corrected for long-chain branching.

The effect of mechanical treatment was determined for resins G-0, H-0, and I-0, using procedures similar to those of Fujiki.[5] Each of the polymers was subjected to mechanical treatment by extruding five successive times. The samples were stored under nitrogen for 48 h and they were then charged to the extruder in a nitrogen atmosphere to prevent thermal-oxidative reactions during extrusion. Extrusion was accomplished on a 36/1 L/D nonvented extruder employing a screw having two mixing sections. Screw speed was 135 rpm and melt temperature was 149 °C. The starting resin and aliquot portions taken after each pass through the extruder were characterized by GPC, by intrinsic viscosity,

Table I
Polymer Characterization and Film Haze Data

polymer desig	melt index, g/10 min	melt index die swell	density, g/cm³	molecular characterization data								total haze,[a] %
				$10^{-4}\bar{M}_n$	$10^{-5}\bar{M}_w$	$10^{-6}\bar{M}_z$	$10^{-3}\langle Mg\rangle_n$	$10^{-3}\langle Mg\rangle_w$	$10^{-3}\langle Mg\rangle_z$	$\bar{M}_z/\bar{M}_w$	$\langle Mg\rangle_z/\langle Mg\rangle_w$	N_w	
A-0	2.28		0.919	1.63	8.16	13.5	11.5	31.9	49.5	16.5	1.55	162	20.9
B-0	1.27			1.69	2.02	1.83	13.1	35.5	53.0	9.06	1.49	24	12.8
C-0	4.19		0.919	1.23	2.12	1.69	9.4	27.5	40.3	7.97	1.47	38	9.2
D-0	1.52		0.922	1.35	1.68	1.20	10.8	32.4	47.3	7.14	1.46	22	6.0
E-0	1.83			1.86	1.32	0.77	14.1	32.4	46.6	5.83	1.44	15	4.5
F-0	1.83		0.926	2.15	1.10	0.36	16.0	32.9	46.4	3.27	1.41	12	3.2
G-0	2.1	1.63	0.919	2.11	7.88	10.1	13.8	32.2	49.4	12.8	1.54	156	21.9
H-0	2.8	1.58	0.919	1.23	1.65	1.45	10.2	33.2	51.2	8.8	1.54	24	8.1
I-0	2.1	1.43	0.922	1.45	1.08	0.40	11.9	33.6	48.9	3.7	1.45	10	5.4
HD-0	1.6	1.52		1.45	1.76	2.31				13.1		nil	50.5

[a] Total haze of blown films.

and by die swell measurements. Nomenclature of these resins is straightforward: G-5 indicates that the polymer was obtained by extruding G-0 five times.

Die swell, d_e/d_c, defined as the ratio of the diameter of the extrudate to that of the capillary, was determined on melt index strands with a micrometer. Die swell recovery experiments were made on Instron capillary rheometer strands, using a 2.54-cm-long and 0.15-cm-diameter capillary at a shear rate of 43.2 s^{-1}. Pellets were stabilized against thermal-oxidative degradation. The pellets were quickly charged to the rheometer and strands were extruded for die swell measurements as soon as temperature equilibration was achieved, i.e., 6 min after charging and periodically thereafter for a time period of 300 min.

Resins A-0 through F-0 were blown into tubular films with a 5-cm film line at the following conditions: 2:1 blowup ratio; 10-cm die diameter and 0.6-mm die gap; 32 rpm extruder screw speed and 18 kg/h output; 185 °C melt temperature; 30-cm frost line distance and 25-μm film thickness. Because of smaller available sample size, polymers G-0, H-0, and F-0 and their mechanically treated derivatives were converted to blown films by using a 2.5-cm blown film line at the following conditions: 2.5/1 blowup ratio; 0.76-mm die gap; 37 rpm extruder screw speed; 12.7-cm frost line distance; 176 °C melt temperature; 30-μm film thickness. On-line measurements were made on flat films extruded at the following conditions, using a 1.9-cm-diameter extruder with 25:1 L/D: 10-cm die width; 0.025-cm die gap; 11.3 rpm extruder screw speed; ~10-cm frost line distance; 180 °C melt temperature; 50-μm film thickness at the center of the film (~75 μm at the edges).

Static haze measurements were made with a Gardner hazemeter following ASTM standard procedure D1003. In our work, haze is defined as the percentage of transmitted light which is scattered in the forward direction at angles between 2.5 and 90°. The precision of this measurement is ~0.2% absolute. A Gardner hazemeter, Model XL100, with the moving film located 2 cm in front of the window to the integrating sphere, was used for on-line haze measurements. The precision of this measurement is ~1% absolute. Equipment similar to that described by Stein and Rhodes, equipped with a continuous-wave He–Ne laser 632.8-nm light source, was used to obtain SALS patterns.[16] In these measurements the plane of polarization of the incident beam was parallel to the machine direction, i.e., extrusion direction, of the film.

A Leitz microscope with differential interference contrast (DIC) optics and an AMR 1000A scanning electron microscope (SEM) were used to examine film surfaces. Films for SEM examination were coated with gold–palladium alloy to reduce electrical charging, and micrographs were obtained from back-scattered electrons. Improved contrast was obtained by tilting the films ~30° with respect to the direction of the incident beam.

Film temperatures were measured with a Temptron Model IT 7288 radiation pyrometer. The instrument was calibrated by adjusting its emissivity setting so that the indicated temperature of the flowing polymer at the die exit equaled the die temperature.

Results and Discussion

The spatial origin of light scattering from films is a key question in determining the mechanism of haze formation. Light scattering from a surface can be virtually eliminated by wetting the surface with a fluid with a refractive index equal to that of the film, 1.51. Haze measurements were made on tubular blown films with two, one, and no surfaces wetted with di-*n*-butyl phthalate. Through such measurements the haze contributions of the interior and the outer surfaces of the tubular blown film were determined. The results for a series of LDPE resins covering a broad range of total haze are shown in Table II.

This table shows that internal haze of the LDPE films is small, 0.2–0.4%, compared to the total haze of 3–21%. This level of internal haze is modestly lower than the 0.5–1.2% values reported by other investigators.[3-5] This is possibly due to the absence of antiblock agents in the resins which we employed. Haze originates very largely from light scattering from the surfaces of the film, with the outer surface of the tubular film contributing a slightly greater amount of haze than the inner surface of the film. Since the outer surface of the film is cooled by an airstream during extrusion, whereas the inner surface is cooled by stagnant air, a difference between the two surfaces is not unexpected. The lower haze contributed by the more slowly cooled inner surface is consistent with Huck and Clegg's view that molten surface bumps smoothen partially before they are frozen-in by solidification of the film,[3] but there may be alternate explanations for this observation.

Table II
Source of Haze of LDPE Blown Films

polymer desig	total haze, %	% contribution from outer surface	% contribution from inner surface	% contribution from interior
A-0	20.9	10.5	10.0	0.2
B-0	12.8	6.7	5.9	0.2
C-0	9.2	5.1	3.9	0.2
D-0	6.0	3.1	2.7	0.2
E-0	4.5	2.3	2.0	0.2
F-0	3.2	1.6	1.4	0.4

Similar measurements on an HDPE blown film, HD-0, showed a higher total haze level, 50.5%, with a surface haze contribution of 43% and an interior haze contribution of 7.5%.

Microscopic Examination. Micrographs of blown LDPE films indicate that haze increases as surface roughness increases. A low-magnification SEM micrograph of the highest haze LDPE film, A-0, shows mounds a few micrometers in diameter (Figure 1). Focusing on the top of mounds and on the bottom of depressions between mounds with a small-depth-of-field objective on an optical microscope equipped for DIC observation revealed that the mounds protruded from the surface by about 1 μm. The SEM micrograph of lowest haze film, F-0, shows that the surface is relatively smooth. The mounds are less evident, and the height of protrusions out of the plane of the surface was found to be much less than 1 μm. We believe that the moundlike features a few micrometers in size seen in these micrographs are the main cause of the haze of high-haze film.

The appearance of the surface of blown HDPE film in the low-magnification DIC micrograph in Figure 1 differs from that of blown LDPE films. Here we see a row-nucleated structure with rodlike features. The rod axes are oriented parallel to the machine direction and are ~3 μm in diameter and greater than 10 μm in length. A row-nucleated morphology is characteristic of many polymers crystallized out of flowing melts.[17]

Higher magnification SEM micrographs of high- and low-haze LDPE films and HDPE film are given in Figure 2. Fibrous-appearing striations oriented perpendicular to the machine direction are observed on the surface of HDPE film. The striations on the rods comprising the row-nucleated structure are spaced at ~0.2 μm, and they are thought to be lamellae packets. The lamellae meet at the lateral rod boundaries, forming depressions oriented parallel to the machine direction. These depressions are believed to be the cause of scattering in the transverse direction in the V_v SALS pattern of this film (see below). The LDPE films also have a lamellar texture, albeit on a finer scale, with lamellae axes preferentially oriented perpendicular to the machine direction. This observation is consistent with SAXS and WAXS patterns of LDPE blown films which show that crystalline lamellae and the *b* axis of the crystal unit cell are preferentially oriented perpendicular to the machine direction. However, the lamellar features of high- and low-haze LDPE films seen in Figure 2 are quite similar. It therefore appears that

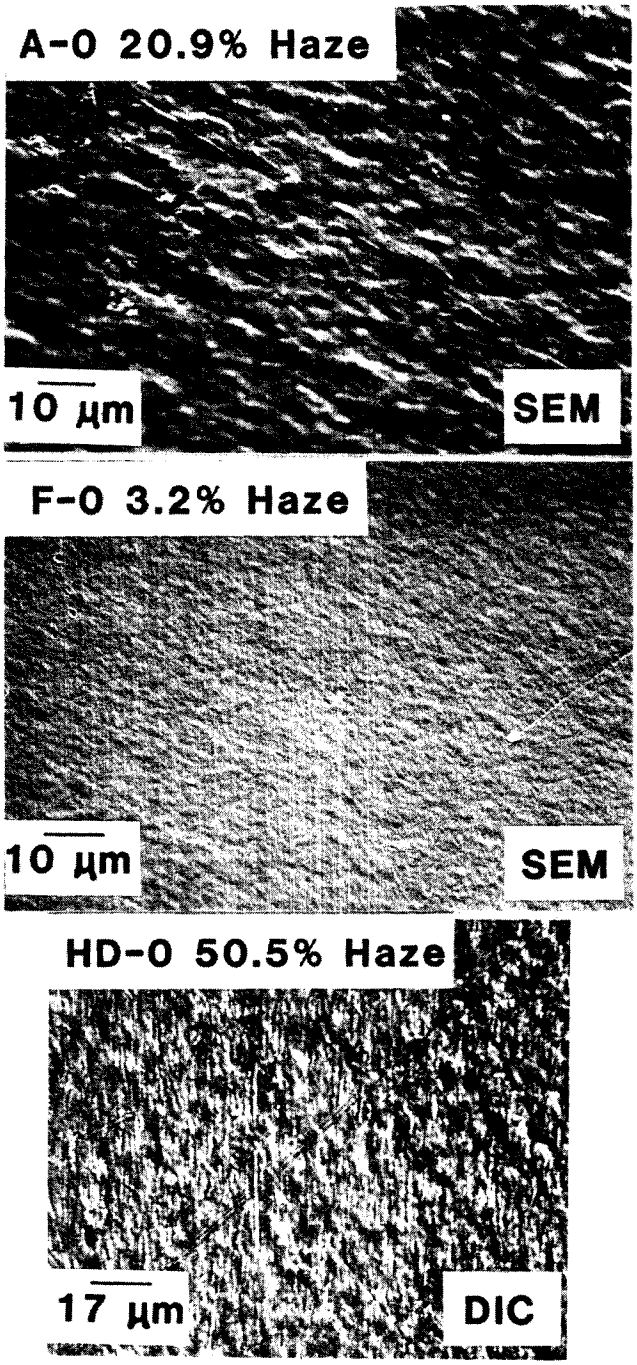

Figure 1. Low-magnification SEM and DIC micrographs of polyethylene blown films. Machine direction is vertical.

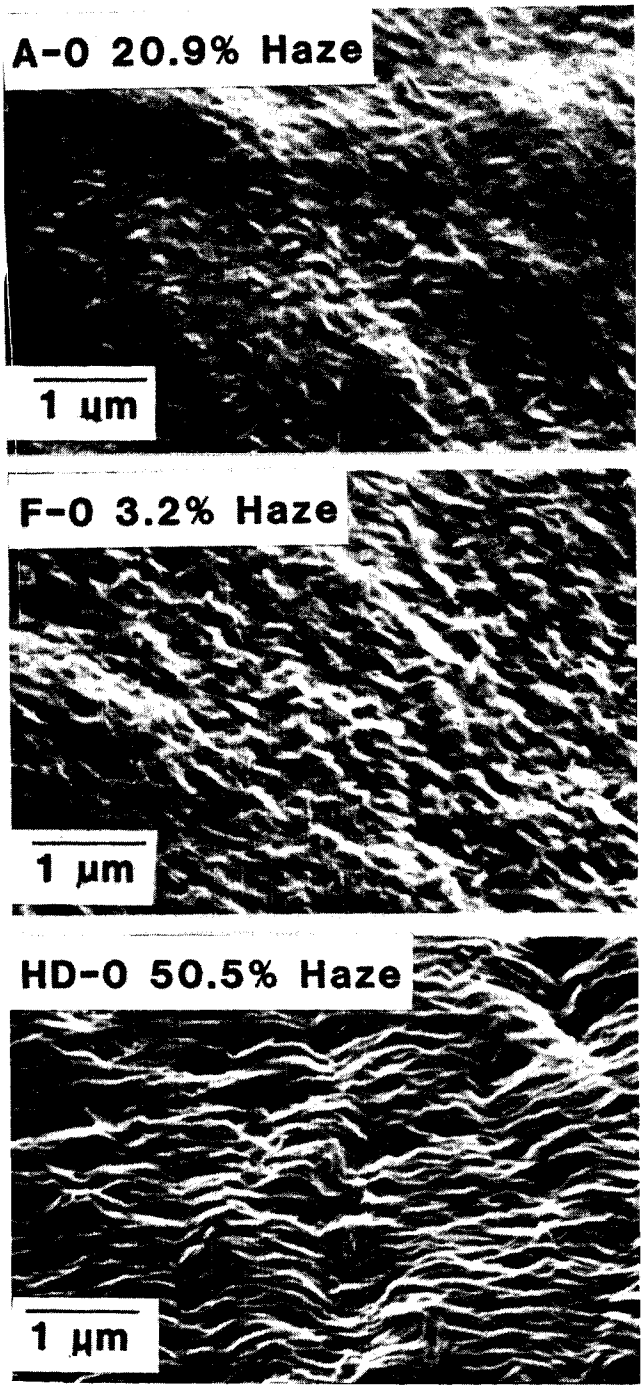

Figure 2. Higher magnification SEM micrographs of polyethylene blown films. Machine direction is vertical.

lamellar features are not the main cause of haze of high-haze LDPE films.

SALS. SALS supports the conclusion that haze is caused very largely by surface scattering. It also provides information concerning the angular distribution of scattered light and the orientation of scattering elements on the film surface.

V_v, H_h, and H_v SALS patterns over an angular range from 0 to 20° from high- and low-haze LDPE films are shown in Figure 3. V_v scattering from the highest haze LDPE film, film A-0, is very intense and lacks circular symmetry. The pattern has the appearance of two lobes having greater intensity in the machine direction than in the transverse direction. However, a partially overlapping four-lobe pattern could have a similar appearance, and it cannot be excluded by our qualitative measurements. The H_h pattern of this film is indistinguishable from the V_v pattern, whereas the H_v pattern has a similar symmetry but is much less intense. These observations show that the scattering comes mainly from density fluctuations rather than from anisotropy and orientation fluctuations. When this film was wetted with di-*n*-butyl phthalate, V_v, H_h, and H_v scatterings were reduced to very low levels. This large diminution in intensity proves that the density fluctuations causing the light scattering are located at the film surface; i.e., the light scattering is caused mainly by surface roughness. The lack of circular symmetry of the V_v and H_h patterns obtained from the dry film shows that the surface irregularities causing these patterns do not have a random orientation.

Scattering patterns from LDPE films with intermediate haze levels are similar to those described above but they are less intense. This trend continues through the lowest

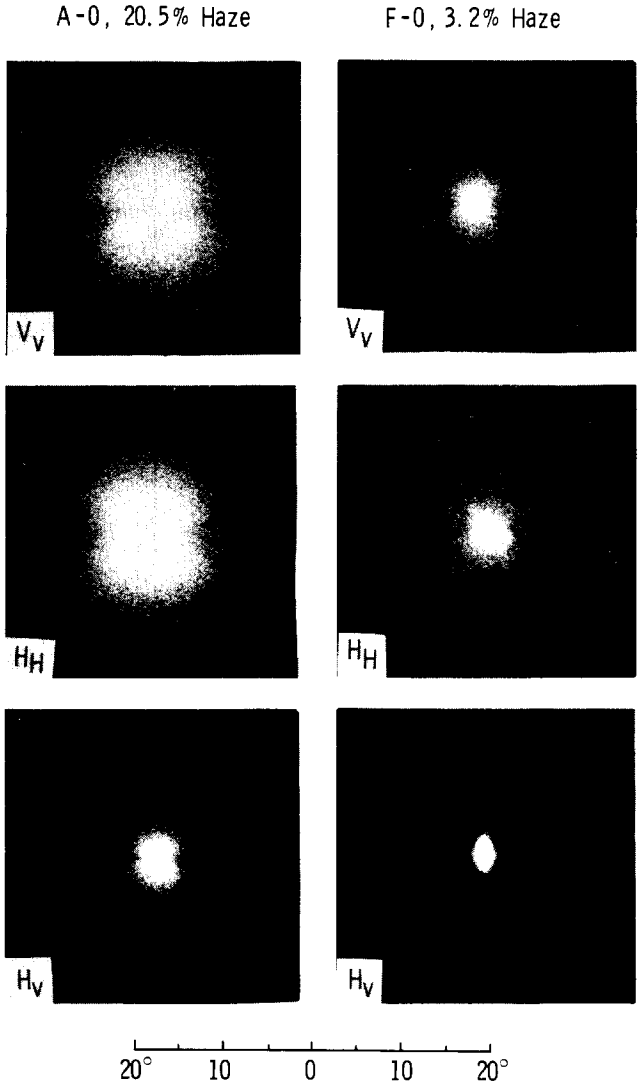

Figure 3. SALS patterns from blown LDPE films. Machine direction is vertical. No fluid on film surface. The H_v pattern was obtained at 25-fold greater exposure than the V_v and H_h patterns.

haze film, film F-0, whose SALS patterns are also shown in Figure 3.

Scattering from HDPE film also comes largely from surface roughness. As shown in Figure 4, V_v and H_h patterns are again much more intense than the H_v pattern. The V_v, H_h, and H_v scattering intensities were again greatly reduced by wetting the film surface. However, the shape of the V_v scattering patterns from HDPE and LDPE films differ. V_v scattering from HDPE is more intense in the transverse direction than in the machine directions. We suggest that this scattering in the transverse direction comes from depressions formed at the rod boundaries of the row-nucleated structures seen on the surface of this film. As noted above, the diameter of the rods is ca. 3 μm. Using the equation for scattering from a periodic linear diffraction grating, $\lambda = d \sin \theta$, and taking the wavelength λ to be 633 nm and the grating period d to be 3 μm yield a scattering angle of 12°. Thus, the separation between rod centers is of the correct order of magnitude to cause scattering in the observed 0–18° range.

The source of the asymmetry of the V_v scattering of high-haze LDPE film is not well understood, however. Scattering from lateral boundaries of rods in row-nucleated structures would scatter light in the transverse direction, whereas the V_v pattern of LDPE films is more intense in the machine direction. Individual lamellae or lamellae packets in row-nucleated structures, on the other hand, are appropriately oriented to scatter light preferentially in the machine direction. However, the observed lamellae spacing for the LDPE films in Figure 2, ~100 nm, is much smaller than the wavelength of light. Scattering from this source should therefore extend to high angles rather than dying away at low angles. Furthermore, the fine-scale lamellar structure in high- and low-haze film is rather similar, so it appears difficult to explain the large difference in scattering intensity on such a basis. We therefore speculatively suggest that the asymmetry of the LDPE V_v scattering is caused by a subtle anisotropy in the shape and arrangement of micrometer-scale mounds on the film surface.

Visual Haze Observations during Blow Film Extrusion. Visual observations of haze at various points downstream from the die during extrusion are consistent with the view that two mechanisms contribute to haze formation.

Visual observations of LDPE films during extrusion show that haze develops in a different manner for low-haze and high-haze films. The low-haze film is very clear to the eye up to about the frost line of the film. The frost line is defined as the point where the diameter of the tube becomes constant. Measurements of film temperature as a function of distance from the die exit describe a cooling curve which displays an exothermic inflection in the vicinity of the frost line. This shows that rapid crystallization occurs in the frost line region. Haze developed in the frost line region is therefore attributed to crystallization

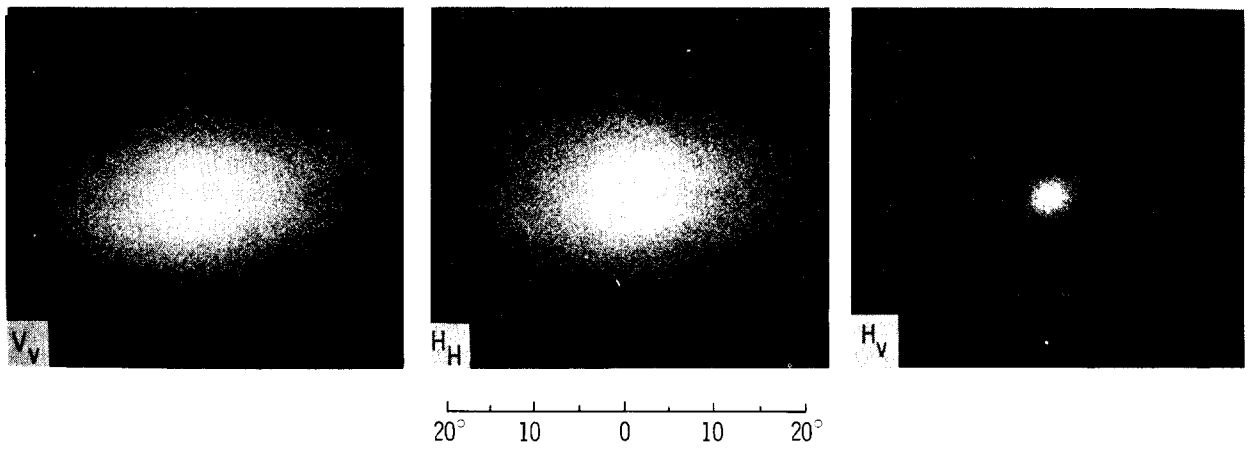

Figure 4. SALS patterns from blown HDPE films with 50.5% haze. Machine direction is vertical. No fluid on film surface. The H_v pattern was obtained at 25-fold greater exposure than the V_v and H_h patterns.

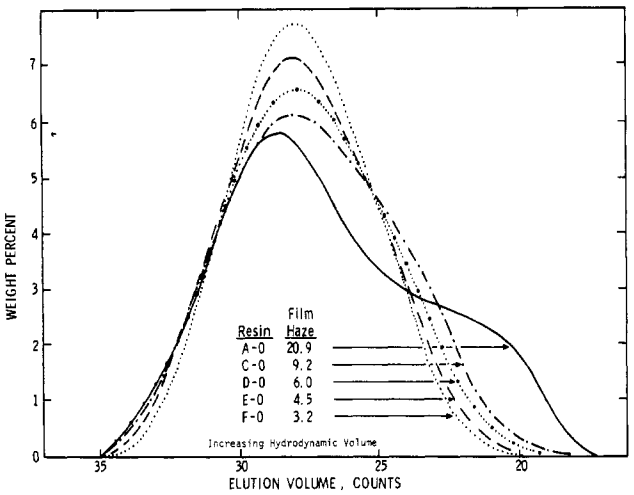

Figure 5. GPC curves of LDPE resins yielding films with various haze levels.

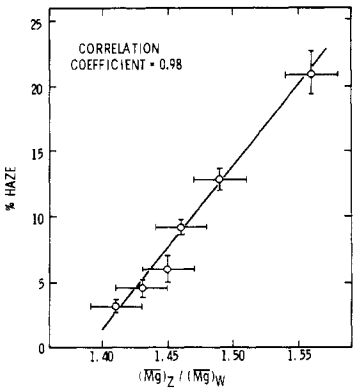

Figure 6. Correlation of total haze of blown LDPE films and molecular size distribution parameter $\langle Mg\rangle_z/\langle Mg\rangle_w$.

processes which cause "crystallization haze" by roughening of the surface of the film. It appears from these qualitative observations that crystallization contributes significantly to haze in low-haze films. Crystallization also causes internal haze; but, as shown previously, the magnitude of the internal haze in our blown films is very small.

In contrast, the high-haze film is very hazy very close to the die exit. Surface roughening in this region is attributed to rheologically induced melt disturbances, i.e., to "extrusion haze" in Huck and Clegg terminology.

Effect of Polymer Chain Structure on Total Haze. The total haze of films listed in Table II is strongly influenced by the relative concentration of large molecules in the polymer. This is apparent from the GPC chromatographs in Figure 5, where elution volume decreases as the "hydrodynamic" volume, $[\eta]M$, of the molecules increases. The correlation between haze and the concentration of large molecules is presented in a quantitative way in Figure 6, where total haze is plotted against a size distribution parameter $\langle Mg\rangle_z/\langle Mg\rangle_w$. The quantity $\langle Mg\rangle$ is related to the hydrodynamic volume and is the mean product of molecular weight, M, and the branching parameter, g, defined by

$$g = \langle S^2\rangle_B/\langle S^2\rangle_L \qquad M_B = M_L$$

where the ratio of $\langle S^2\rangle_B$ to $\langle S^2\rangle_L$ compares the mean-square radii of gyration for long-chain branched molecules and linear molecules of the same molecular weight. The mean product $\langle Mg\rangle$ is proportional to $\langle S^2\rangle$ and is derived from GPC–intrinsic viscosity measurements.[14,15] The ratio $\langle Mg\rangle_z/\langle Mg\rangle_w$ heavily weights the large-size molecules in the molecular size distribution. As the concentration of large-size molecules increases, $\langle Mg\rangle_z/\langle Mg\rangle_w$ increases. The close correlation between total haze and this size distribution variable is indicated by the high correlation coefficient, 0.98. A good correlation is also obtained between haze and the molecular weight distribution parameter $\bar{M}_z/\bar{M}_w$ (correlation coefficient 0.97) and a fair correlation is obtained with N_w, the number of long branches in a weight-average molecule (correlation coefficient 0.89). The three structure variables $\langle Mg\rangle_z/\langle Mg\rangle_w$, $\bar{M}_z/\bar{M}_w$, and N_w are strongly correlated in these samples; however, even though it is clear that large molecules have a major influence on haze level, additional work on a larger set of judiciously selected polymers is required to determine the controlling structural features.

In anticipation of results discussed later, we note that mechanical treatment of the polymer melt before film blowing can cause large reductions in haze with no detectable changes in the structure of polymer chains. Consequently, we emphasize that the excellent correlations between haze and the structure variables discussed above would not have been obtained if the selected resins had not all had identical deformation histories.

Huck and Clegg have show that blown film haze increases as polymer melt elasticity increases.[3] The increase in total haze caused by high concentrations of large molecules that we have found is attributed mainly to their effect in increasing melt elasticity. The close relation between melt elasticity and haze is illustrated by the experiments described below on the effect of mechanical treatment on haze.

Effect of Mechanical Treatment. The foregoing results are consistent with the view that there are two causes of haze, i.e., extrusion haze and crystallization haze. We have taken two approaches to obtain additional evidence for the existence of such mechanisms and to estimate the contribution that each mechanism makes to total haze. The first of these approaches involved an examination of the effect of mechanical treatment of the polymer melt on melt rheology and total film haze. The second approach involved making on-line haze, LALS, and temperature measurements during film fabrication, using primarily resins that had been subjected to mechanical treatment.

Additional objectives of the mechanical treatment investigation were to (1) determine the extent that haze can be reduced by mechanical treatment, (2) determine what types of LDPE resins are most susceptible to haze reduction by mechanical treatment, and (3) determine whether haze reduction is caused by chemical effects such as chain scission and cross-linking or by a physical effect. Physical effects include mechanisms such as changing the state of mixing of dissimilar molecular clusters and changing the state of entanglement of the system.

The effect of mechanical treatment was investigated for three LDPE resins. As described in detail in the Experimental Section, these polymers were extruded five times under conditions of rigorous oxygen exclusion. After each pass through the extruder, an aliquot portion was characterized by structural and die swell measurements, and another aliquot portion was made into film. As illustrated by the representative data for resins G-0 and G-5 in Figure 7, careful GPC characterization showed there was no detectable difference in polymer chain structure of the resins before and after repeated extrusion.

As shown in Figure 8, film haze decreased for all samples as a result of mechanical treatment, with most of the haze reduction occurring in the first two extrusions. Because there were no detectable changes in polymer chain struc-

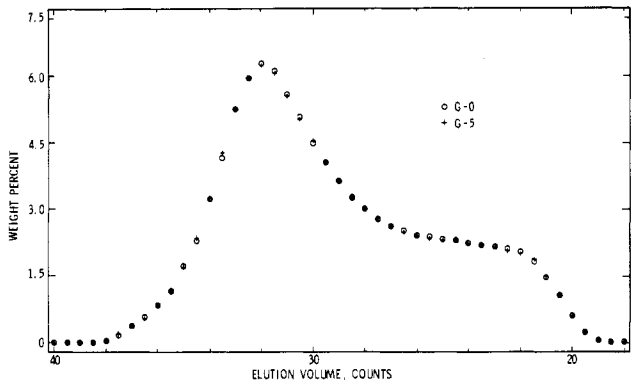

Figure 7. GPC curves of resin G-0 and its multiply extruded analogue G-5.

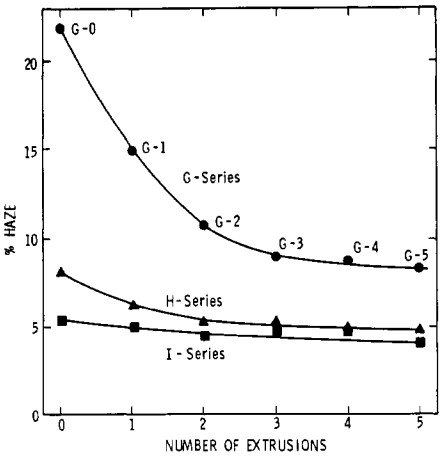

Figure 8. Effect of repeated extrusion of LDPE resins on haze of blown films.

ture during the repeated extrusions, the reduction in haze is attributed to a physical mechanism such as mixing or chain disentanglement. This conclusion confirms Fujiki's contention that mechanical treatment reduces haze by a physical mechanism,[5] and it is in disagreement with the undocumented assertion that haze reduction resulting from mechanical treatment is caused by polymer chain cleavage.[8]

Figure 8 also shows that the susceptibility of the LDPE resins to haze reduction by mechanical treatment differs from one resin to another. For example, the haze of film from the highest haze LDPE polymer, G-0, is greatly reduced by successive extrusions, whereas the haze of film from the lowest haze LDPE polymer, I-0, is reduced only slightly. These observations indicate that the structural features that control the haze level of untreated LDPE polymers also control their susceptibility to haze reduction by mechanical treatment.

Rheological properties of these resins were also affected by mechanical treatment. Melt index swell, a measure of elasticity, changed with successive extrusions as shown for these resins in Figure 9. Swell decreased after the first several extrusions and then leveled off. The magnitude of the reduction in swell decreased in the order G-0, H-0, I-0. Comparisons of Figures 8 and 9 confirm Fujiki's conclusion that the magnitude of the decrease in swell for the LDPE resins parallels the haze reduction obtained on the films blown from the mechanically treated resins. The 22% reduction in swell of G-0 upon mechanical treatment should be considered to be a large change in this property, insofar as the swell of numerous commercial and experimental LDPE resins that we have examined differ by no more than about 50%.

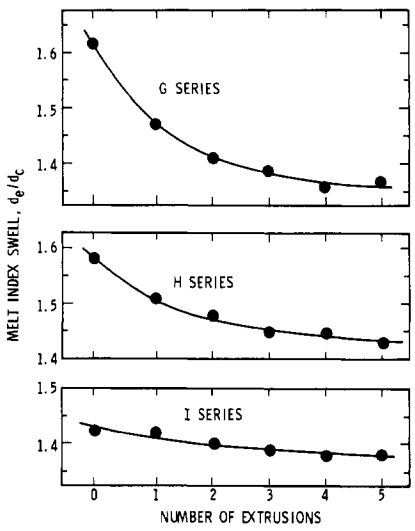

Figure 9. Effect of repeated extrusion on melt index swell of LDPE resins.

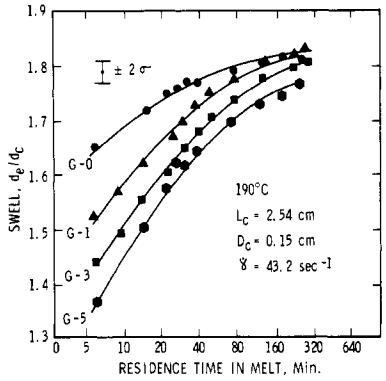

Figure 10. Swell recovery of G series LDPE samples.

Table III
Effect of Mechanical Treatment on Melt Index

no. of extrusions	melt index, g/10 min 0	1	2	3	4	5	% increase in melt index after five extrusions
resin							
G series	2.10	2.60	2.53	2.60	2.69	2.70	29
H series	2.80	2.92	3.04	3.11	3.14	3.21	15
I series	2.06	2.10	2.14	2.16	2.18	2.20	7

In agreement with other investigators,[11,12] mechanical treatment also increases melt index. The initial melt index of each resin prior to repetitive extrusion, together with the percentage increase in melt index after five extrusions, is listed in Table III. For extrusions through low L/D capillary dies, as is the case in the melt index measurement, both viscous and elastic properties of the melt determine the observed flow rate. As a result of the reduction of elasticity by mechanical treatment, a larger portion of the applied shear stress is used for flow. This is at least partly the reason that melt index increases as melt elasticity (swell) decreases. On the basis of preliminary experiments, we believe that viscosity is also slightly reduced by mechanical treatment.

Swell Recovery of Mechanically Treated LDPE. Swell recovery experiments on mechanically treated resins provide further evidence that the changes in haze, elasticity, and melt index obtained on mechanical treatment are not caused by bond cleavage or cross-linking. These experiments also show that mechanical treatment generates a nonequilibrium melt structure that is long-lived at

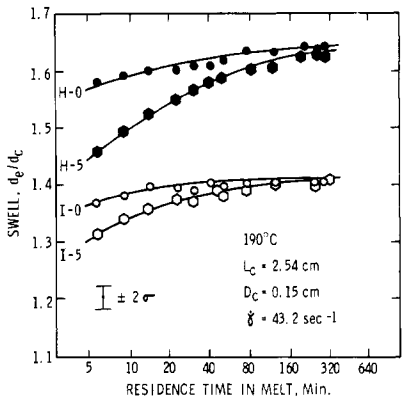

Figure 11. Swell recovery of H and I series LDPE samples.

typical processing temperatures.

In the die swell recovery experiments, die swell was measured as a function of residence time in the melt. The results for the G series of samples are shown in Figure 10, where swell is plotted against the logarithm of the residence time in the melt state at 190 °C. Analogous data for the H and I series of samples are given in Figure 11. These figures show that die swell is not constant with residence time but that it increases toward a limiting value over a period of several hours. For each of the three series, the swelling of the untreated polymer and the mechanically treated polymer converges to the same swell value. This convergence shows that the reduction in swell by mechanical treatment was not caused by a chemical process such as bond cleavage or cross-linking. Rather, the reduction in swell must have been caused by a reversible physical mechanism, such as a change in the state of mixing or a change in the state of entanglement of the system.

Data on die swell recovery at 120 °C obtained on G-5 showed that the approach to an equilibrium melt structure is substantially slower at lower temperatures. Because the recovery times at 120 to 190 °C are long compared with residence times in extrusion equipment, the benefits of reduced melt elasticity obtained by mechanical treatment can be realized in practical processing operations such as the film-blowing process.

It is important to note in Figures 10 and 11 that the swell of the starting resins G-0, H-0, and I-0 increases with residence time in the melt. This behavior shows that these resins, which were not purposely subjected to mechanical treatment, are nevertheless in a nonequilibrium melt state. Two possible explanations for this fact are (1) the observed nonequilibrium state of the starting resins is generated during manufacture upon passage from the high-pressure ethylene reactor to the lower pressure ethylene gas separator, and (2) the observed nonequilibrium state of the starting resins is the result of mechanical treatment received in the melt extruder that follows the gas separator. Fujiki suggested, without giving supporting data, the first of these two possibilities.[5] However, our calculations and experiments support the second explanation. An estimate of the temperature coefficient of swell recovery from measurements at 190 and 120 °C was used to make a rough calculation of the time required for complete swell recovery at the temperature of the polymer melt in the ethylene gas separator. It was estimated that complete swell recovery of the pure melt would take place in less than 30 s. The substantial amount of ethylene dissolved in the polymer would further shorten the time for complete swell recovery. Melt residence times in ethylene gas separators are long compared to 30 s, so equilibration of the polymer melt

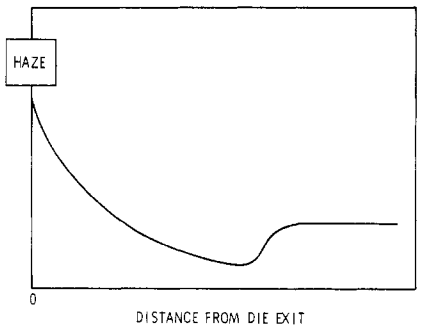

Figure 12. Authors' schematic illustration of haze as a function of distance from die as postulated by Huck and Clegg.[3]

structure should be achieved in the separator before extrusion. Measurements on polymer sampled directly from the gas separator indeed showed that swell did not change with melt residence time in the rheometer. We therefore conclude that the nonequilibrium state of the starting resins arises from mechanical treatment which the resin receives in the melt extruder.

The demonstration that polymers not purposely subjected to mechanical treatment can, nevertheless, have nonequilibrium melt structures has important implications for establishing chain structure–property relationships. For example, two polymers having identical chain structures could have substantially different properties if one were in an equilibrium melt state and the other were not. In attempting to establish chain structure–property relationships, it is, therefore, desirable for all of the polymers examined to be in an equilibrium state or, perhaps less desirably, for all of them to depart from the equilibrium state to the same extent. Otherwise, an imprecise correlation will be obtained, and a correlation could conceivably be completely obscured. Die swell recovery measurements on a limited number of LDPE polymers from several commerical sources show that they are indeed in a nonequilibrium state. The possibility that correlations between chain-structure and polymer properties can be upset by the effects of mechanical treatment has also been suggested by Howells and Benbow[9] and by Rokudai and Fujiki.[18]

On-Line Haze Measurements. Huck and Clegg have suggested that haze would change as a function of distance from the die as illustrated schematically in Figure 12.[3] According to this scheme, extrusion haze developed at the die exit should decrease as the fluid moved downstream because of smoothening of the molten surface. Further downstream, haze should increase as a result of crystallization. On this basis, on-line haze measurements, where haze is measured as a function of distance from the die, would provide a means for estimating the individual contributions that the extrusion haze and crystallization haze mechanisms make to the total haze.

On-line haze measurements could not be made on blown films because the tubular geometry interfered with the measurement. Consequently, on-line haze measurements, as well as SALS, film width, and film temperature measurements, were made on flat films extruded from a slit die. We believe that mechanisms of haze formation are similar for the two types of films. This belief is based in part on the fact that there was a good correlation between haze levels of the two types of films made from the same resins (correlation coefficient 0.94). Furthermore, micrographs of surfaces and SALS patterns were very similar. These similarities are not surprising because the longitudinal melt deformation is much greater than the lateral deformation for both the blown and the flat films. Thus,

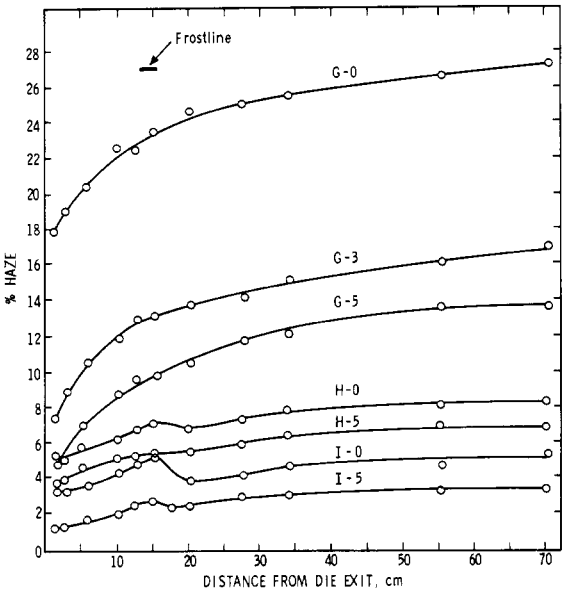

Figure 13. Haze of films as a function of distance from die exit.

the blown films extended longitudinally by a factor of 15 and they expanded laterally by a factor of 2 in the film-forming operation, whereas the flat films extended longitudinally by a factor of about 10 and they contracted laterally by a factor of about 2 during fabrication. However, flat films had larger internal haze values than blown films, 1–2% compared to 0.2–0.4%. This difference in internal haze is probably caused by different cooling rates and different film thicknesses.

On-line haze measurements are given in Figure 13, where haze is plotted against distance from the die exit. The frost line region is also indicated in the figure. It is apparent from this figure that the postulated initial decrease in haze does not occur in these films or in others that we have examined. For example, the haze of G-0 is high at the die exit, and it rises monotonically to a higher level. The shape of the curve for G-3, the thrice-extruded analogue of this film, is similar, but it is displaced to lower haze levels. The curve for G-5 occurs at still lower levels.

Table IV
Variations in Haze with Distance from Die

film	haze close to die exit H_0, %	haze far downstream from die H_∞, %	increase in haze $H_\infty - H_0$, %
G-0	17.8	27.1	9.3
G-3	7.4	16.7	9.3
G-5	4.9	13.7	8.8
H-0	5.3	8.3	3.0
H-5	3.8	7.0	3.2
I-0	3.4	5.2	1.8
I-5	1.2	3.5	2.3

To facilitate the quantitative comparison of such curves, we designate the haze value measured very close (1.3 cm) to the die exit as H_0 and the value measured far downstream from the die (70 cm) as H_∞. H_0, H_∞, and the increase in haze between these two points, $H_\infty - H_0$, are listed in Table IV for the G, H, and I series of films. In the G series there is a large decrease in H_0 upon mechanical treatment, with H_0 decreasing from 17.8% for G-0 to 4.9% for G-5. In both the H and I series there is a similar trend, but the decrease in H_0 is much smaller. Thus, the magnitude of the decrease in H_0 parallels the decrease in elasticity (die swell) of mechanically treated resins. It has long been recognized that the elasticity in polymer melts causes various types of extrusions defects,[9,19] including microscale extrudate distortions. Analogously, the haze developed immediately upon exit from the die, which we identify with extrusion haze, is caused by a microscale (~1 μm) surface roughness generated by an elasticity-dependent process.

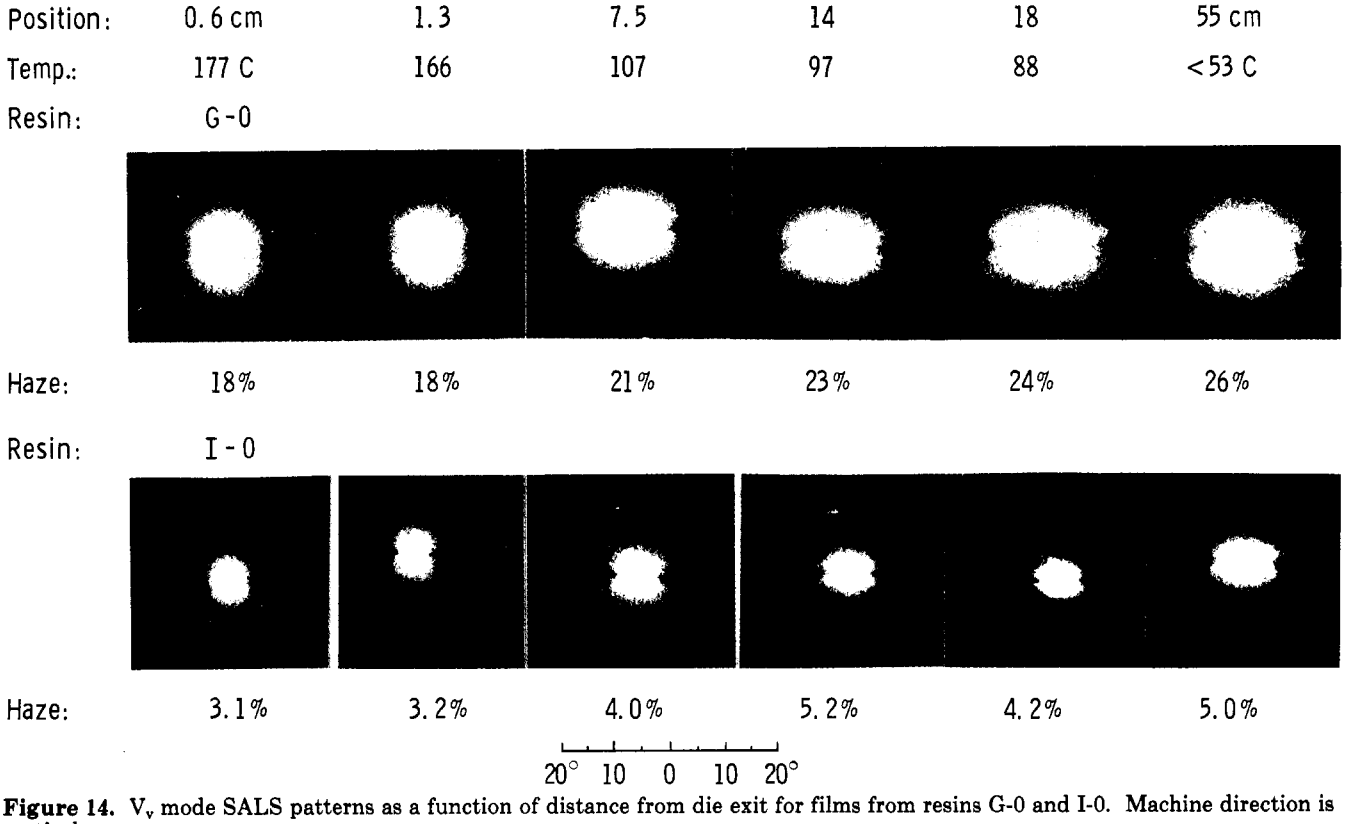

Figure 14. V_v mode SALS patterns as a function of distance from die exit for films from resins G-0 and I-0. Machine direction is vertical.

In contrast to the progressive decrease in H_0 with mechanical treatment, $H_\infty - H_0$ is not affected by mechanical treatment within the precision of the measurement. For example, whereas H_0 values of G-0, G-3, and G-5 are 17.8, 7.4, and 4.9%, respectively, the corresponding $H_\infty - H_0$ values are 9.3, 9.3, and 8.8%. The invariance of $H_\infty - H_0$ with mechanical treatment shows that crystallization haze and other conceivable mechanisms that might be proposed to cause haze in this region are not affected by mechanical treatment.

The reason that haze increases rather than decreases after exit from the die is not well understood. Spatial rearrangement of the surface features generated at the die exit could possibly cause an increase rather than a decrease in haze. The observed change in the symmetry of V_v SALS from an initial cylindrically symmetrical pattern at the die exit to a nonsymmetrical one shortly downstream therefrom (see below) is consistent with such an interpretation. Surface roughening by crystallization must also contribute to the magnitude of $H_\infty - H_0$. The possibility that some unknown mechanism can also contribute to the increase in haze after exit from the die cannot be excluded.

As illustrated by the curve for the I-0 in Figure 13, haze passes through a maximum in the frost line region for some low-haze films. The maximum is more pronounced in some other films we have examined. In examining the bulk crystallization of polyethylene from quiescent melts, Rhodes and Stein found that the intensity of scattered light passed through a maximum during crystallization.[20] The maximum was achieved when spherulites had grown to a size comparable to the wavelength of light and when they pervaded about half of the volume of the sample. In our case, however, the haze maximum is caused by surface scattering. This was demonstrated by placing di-*n*-butyl phthalate onto the surfaces of the film during extrusion in the region of the frost line, whereupon haze immediately decreased to a low value. The increase in haze seen before the frost line region in Figure 13 is thought to be caused by an increase in the number and size of surface bumps in this region. When the number and size of the bumps become sufficiently large, destructive interference occurs, leading to the peak in haze observed in the frost line region for the lower haze samples.

To obtain low-haze film it is necessary that both H_0 and $H_\infty - H_0$ be small. As shown above, H_0 can be reduced by reducing polymer melt elasticity, but the factors that affect $H_\infty - H_0$ are not so apparent. It would be desirable to make on-line measurements on a larger number of resins to establish a correlation between $H_\infty - H_0$ and molecular structure. However, such extensive measurements have not been made, and improvement in the precision of on-line haze measurements would be necessary to obtain a good correlation with molecular structure.

On-Line SALS Measurements. SALS measurements during film extrusion show changes in the angular distribution of scattered light that must be explained by proposed haze mechanisms. V_v-mode SALS patterns, as well as haze and film temperatures, at various points downstream from the die are shown in Figure 14. The scattering pattern of the high-haze film G-0 at 0.6 cm from the die is very intense and almost circularly symmetric. Quickly, thereafter, a double-lobe pattern develops whose spatial extent increases upon moving farther away from the die. H_v scattering was very weak and is not shown. Scattering from the mechanically treated analogue of this resin, G-5, was similar to that of G-0 at equivalent positions, but scattering was less intense. The intensity of light scattering from the low-haze film I-0 is much less than that from G-0, but the symmetry is similar (see Figure 14). As discussed above, this film has a haze maximum in the frost line region. Consistent with this observation, the SALS pattern has a smaller spatial extent at 1.3 and 18 cm than at 7.5 and 14 cm from the die. Uninterpreted on-line SALS patterns of HDPE films reported by others also show a double-lobe pattern that is more intense in the frost line region than on either side.[21]

A distinctive feature of the V_v-mode SALS scattering is that it is nearly circularly symmetric very close to the die. This indicates that the surface bumps have a random orientation on the surface very close to the die exit. A short distance from the die, where the indicated temperature is about 166 °C, the double-lobe scattering first appears. This basic pattern persists throughout the process, usually with gradually increasing intensity.

As discussed previously, the characteristic double-lobe V_v scattering from LDPE films can be attributed to a subtle anisotropy in the arrangement of micrometer-scale mounds on the film surface. Any interpretation of this pattern in terms of crystallization effects, such as scattering from lamellae boundaries on the film surface, should be tempered by the fact that the double-lobe patterns first appear at an indicated temperature of ~165 °C, which is much higher than the ~100 °C quiescent crystallization temperature of LDPE. Of course, crystallization from flowing oriented melts occurs at higher temperatures than from unoriented melts.[22] However, even at high takeup speeds the crystallization temperature of HDPE fibers is less than 166 °C,[22] so it is improbable that the crystallization temperature of LDPE could be raised to 170 °C under our extrusion conditions. This difficulty could be rationalized by the suggestion that radiation pyrometry measures an average temperature over a considerable depth into the film; i.e., it effectively measures an average bulk temperature. The temperature within a micrometer or so from the film–air interface might then be considerably lower than the indicated temperature, thus allowing crystallization to occur at the surface. The validity of this rationalization can be tested by temperature profile calculations. However, such calculations require a knowledge of the infrared transmission of the pyrometer and molten polymer[23] and they have not been made.

Considering further the crystalline contribution to the total haze: if lamellae organized into larger superstructures were the main cause of crystallization-caused surface roughening, then it would be desirable to thwart the formation of such structures to reduce haze. Mandelkern recently concluded that a random organization of lamellae, in contrast to a correlated arrangement of lamellae into a larger superstructure, is favored by a high concentration of structural irregularities, such as comonomer units or short-chain branches.[24] Reduction of the size of the superstructure would also reduce the small contribution that internal haze makes to the total haze. The very low haze levels of poly(ethylene-*co*-vinyl acetate) films, ~3% under our film-blowing conditions, is consistent with this possibility.

Notwithstanding the present uncertainty in the detailed interpretation of on-line SALS measurements, this technique is potentially very useful because it is one of the few available methods for examining surface topography as it develops during film formation.

Conclusions

The static and dynamic measurements described above show that haze of LDPE film is caused very largely by light scattering from the rough film surfaces. Our results confirm Huck and Clegg's hypothesis that there are at least

two mechanisms causing surface roughening and surface haze, namely, (1) extrusion haze, which results from flow disturbances at the die exit caused by the elastic nature of the polymer melt, and (2) crystallization haze, which results from stress-induced crystallization close to the film surface.

To obtain low-haze film it is necessary to reduce both extrusion haze and crystallization haze. Extrusion haze can be reduced by selecting polymers which contain a relatively low concentration of large molecules and by intensive mechanical deformation of the melt prior to film extrusion. Mechanical treatment reduces elasticity and film haze by a reversible physical mechanism that generates a long-lived nonequilibrium melt structure, rather than by a chemical mechanism involving chain cleavage and cross-linking. The relaxation time toward the equilibrium melt structure is long compared to typical residence times in extrusion equipment, so the benefits of reduced melt elasticity obtained by mechanical treatment can be realized in practical processing operations such as the film-blowing process. The effect of mechanical treatment must also be considered in developing correlations between polymer chain structure and physical properties.

The detailed mechanism by which crystallization causes surface roughening is not so well understood, and methods for reducing crystallization haze are not so apparent. However, increasing the structural irregularity of the polymer chains probably reduces crystallization-caused surface roughening, and it probably also reduces internal haze to yet lower levels.

References and Notes

(1) Stein, R. S. In "Structure and Properties of Polymer Films"; Lenz, R. W., Stein, R. S., Eds.; Plenum Press: New York, 1973; p 1.
(2) Hashimoto, T.; Todo, A.; Murakimi, Y.; Kawei, H. *J. Polym. Sci., Polym. Phys. Ed.* **1977**, *15*, 501.
(3) Huck, N. D.; Clegg, P. L. *SPE Trans.* **1961**, *1*, 121.
(4) Perron, P. J.; Lederman, P. D. *Polym. Eng. Sci.* **1972**, *12*, 340.
(5) Fujiki, T. *J. Appl. Polym. Sci.* **1971**, *15*, 47.
(6) Foster, G. N. *Polym. Prepr., Am. Chem. Soc., Div. Polym. Chem.* **1979**, *20*, 463.
(7) Shroff, R. N.; Cancio, L. V.; Shida, M. *Polym. Eng. Sci.* **1977**, *17*, 796.
(8) Albright, L. F. *Chem. Eng. (N.Y.)* **1966**, *73*, 113.
(9) Howells, E. R.; Benbow, J. J. *Trans. J. Plast. Inst.* **1962**, *30*, 240.
(10) Rokudai, M. *J. Appl. Polym. Sci.* **1979**, *23*, 463.
(11) Prichard, J. H.; Wissbrun, K. F. *J. Appl. Polym. Sci.* **1969**, *13*, 233.
(12) Hanson, D. F. *Polym. Eng. Sci.* **1969**, *9*, 405.
(13) Drott, E. E.; Mendelson, R. A. *J. Polym. Sci., Part A-2* **1970**, *8*, 1361.
(14) Westerman, L.; Clark, J. C. *J. Polym. Sci., Polym. Phys. Ed.* **1973**, *11*, 559.
(15) Chung, C. I.; Clark, J. C.; Westerman, L. In "Advances in Polymer Science and Engineering"; Pae, K. D., Morrow, D. R., Chen, Yu, Eds.; Plenum Press: New York, 1972; p 249.
(16) Stein, R. S.; Rhodes, M. B. *J. Appl. Phys.* **1960**, *31*, 1873.
(17) Peterlin, A. *Polym. Prepr., Am. Chem. Soc., Div. Polym. Chem.* **1975**, *16*, 315.
(18) Rokudai, M.; Fujiki, T. *J. Appl. Polym. Sci.* **1979**, *23*, 3295.
(19) Bagley, E. B.; Schreiber, H. P. In "Rheology"; Eirich, F. R., Ed.; Academic Press: New York, 1969; Vol. 5, p 93.
(20) Rhodes, M. B.; Stein, R. S. *J. Polym. Sci.* **1960**, *45*, 521.
(21) Nagasawa, T.; Matsumura, T.; Hoshio, S. *Appl. Polym. Symp.* **1973**, *20*, 295.
(22) Spruiell, J. E.; White J. L. *Polym. Eng. Sci.* **1975**, *15*, 660.
(23) Dahl, A. I., Ed. "Temperature, Its Measurement and Control in Science and Industry"; Reinhold: New York, 1962; Vol. 3, Part 2, p 381.
(24) Mandelkern, L.; Maxfield, J. *J. Polym. Sci., Polym. Phys. Ed.* **1979**, *17*, 1913.

Dynamic Small-Angle X-ray Scattering Studies on Diffusion of Macromolecules in Bulk. 2. Principle and Preliminary Experimental Results†

Takeji Hashimoto,* Yasuhisa Tsukahara,‡ and Hiromichi Kawai

Department of Polymer Chemistry, Faculty of Engineering, Kyoto University, Kyoto 606, Japan.

Received October 2, 1980

ABSTRACT: We discuss the change in X-ray, light, and neutron elastic scattering intensity distributions with time when phase-separated structures in block polymers or polymer blends are transformed into a homogeneous mixture by suddenly removing the thermodynamic driving force for the phase separation, e.g., by a temperature jump. During the phase separation the intensity decays exponentially with time at a rate depending on a diffusion coefficient D_c for the center-of-mass motion of the molecules in bulk and q^2, where $q = (4\pi/\lambda) \sin(\theta/2)$ is the scattering vector, which provides a possible approach for evaluating D_c for the self-diffusion. As an application, we evaluated the activation energy (13 kcal/mol) for the diffusion of a particular block polymer of styrene and isoprene by the small-angle X-ray scattering technique, the result of which is consistent with values estimated from rheological measurements.

I. Introduction

Rheological properties of bulk polymers in melts are greatly affected by the molecular entanglements in the system because the entanglements affect the molecular motion.[1] Studies on the translational diffusion of polymer molecules in bulk would be especially of value and provide important information on the physics of entangled systems.[1-3] For example, a classical entanglement-coupling model proposed by Bueche[4] predicts the translational diffusion coefficient D_c for the center-of-mass motion of polymer molecules in bulk to be given by

$$D_c \propto M^{-3.5}$$

† Part 1 of this series corresponds to ref 17.
‡ Present address: Department of Synthetic Chemistry, Faculty of Engineering, Nagoya University, Nagoya 464, Japan.

0024-9297/81/2214-0708$01.25/0